Supporting Information for

Intramolecular Hydrogen Bonding: A Key Factor Controlling Photosubstitution of Ruthenium Complexes

Masanari Hirahara*[a], Hiroyuki Nakano, Kyohei Uchida [a], Rei Yamamoto [a], and Yasushi Umemura [a]

Department of Applied Chemistry, School of Applied Science, National Defense Academy of Japan, Hashirimizu 1-10-20, Yokosuka, Kanagawa, 239-8686

E-mail: hirahara@nda.ac.jp

Supporting Information

Contents

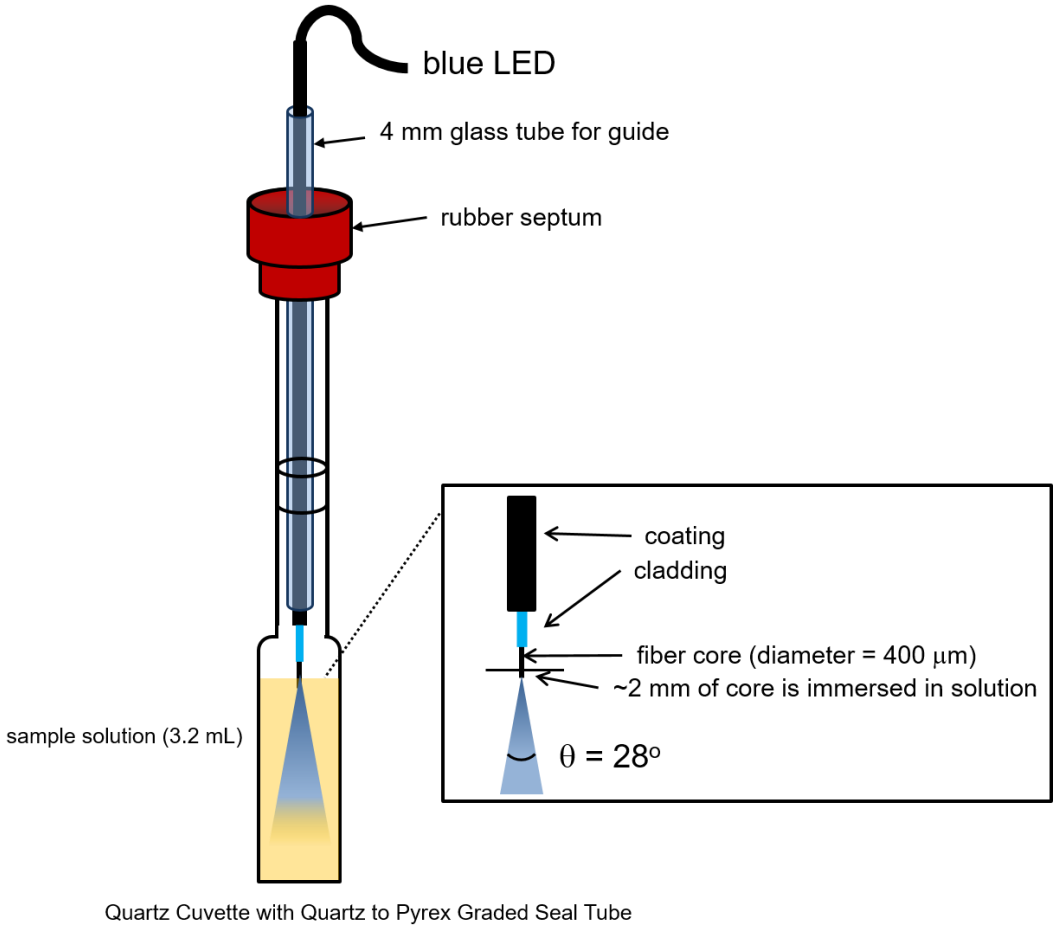

Figure S1. Experimental setup for the photosubstitution experiments with blue LED.

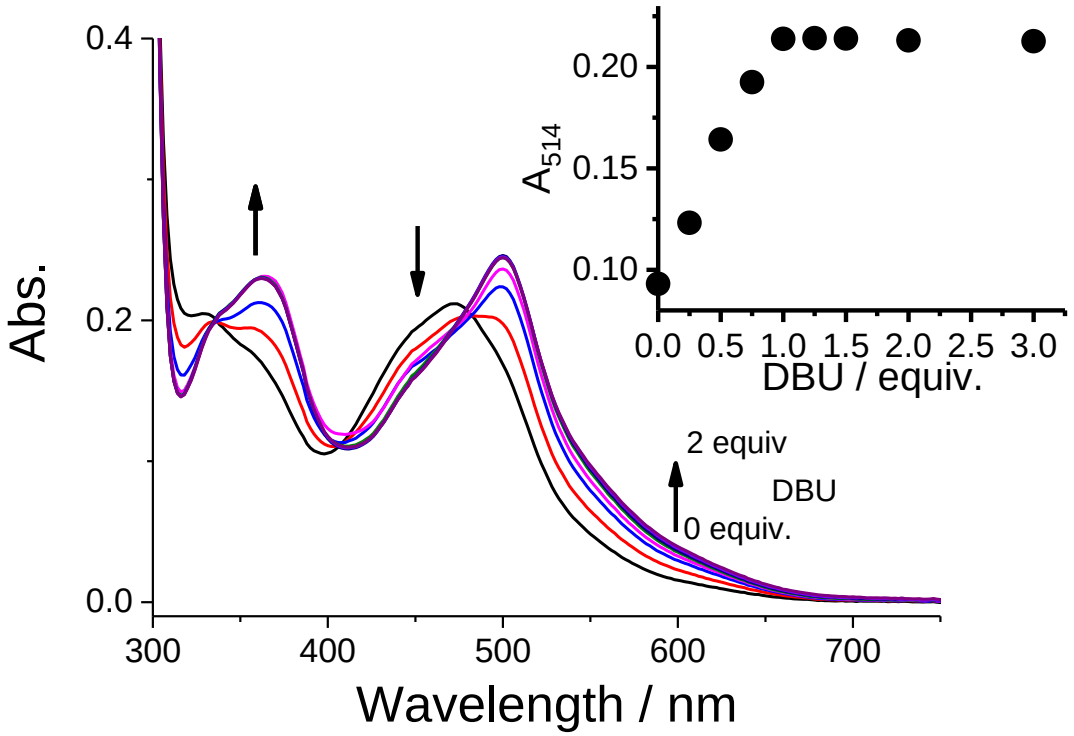

Figure S2. Absorption spectral changes of **1a** during the titrtation eximeriments with DBU as a base. Inset shows the changes of absorption at 514 nm upon the addition of DBU. The absorption maxima (500 nm) of mono-deprotonated complex **1b** coincides with the reported value.[1] Absorption spectra upon addition of excess amount of DBU are shown in Figure S5.

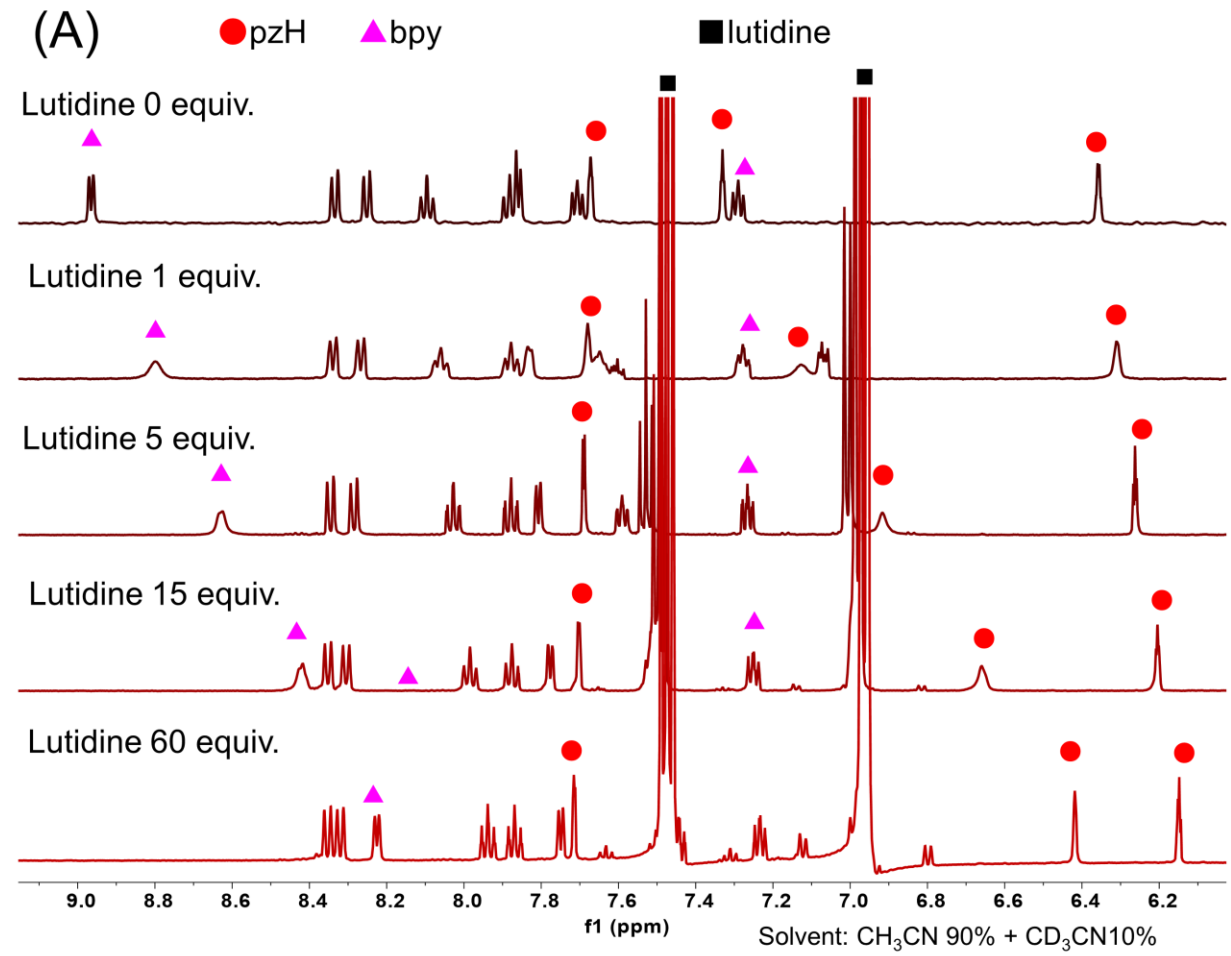

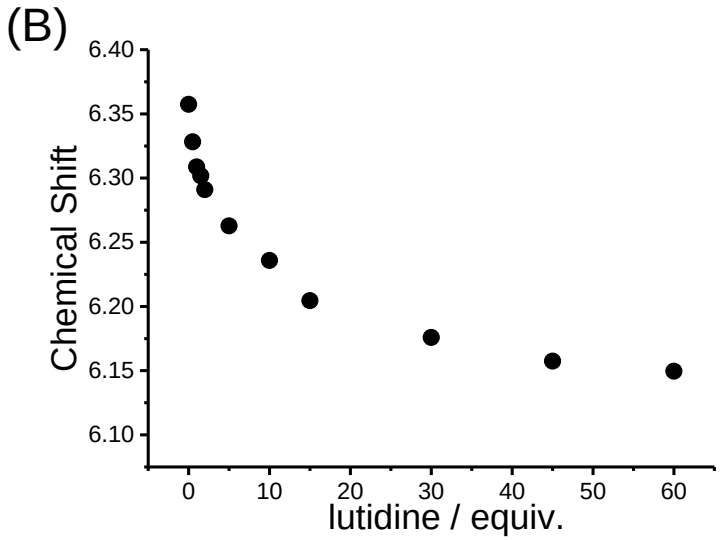

Figure S3. (A) ^{1}H NMR spectra of **1a** (5 mM) during the titration experiment with lutidine (pK_a = 14.13 in acetonitrile[2]) in 90 % CH_3CN and 10 % CD_3CN. (B) Plots of chemical shift of a singlet peak at 6.36 ppm upon the addition of lutidine. (C) Titration plot for deprotonation of **1a** to **1b** upon addition with lutidine.

Figure S3. (Continued)

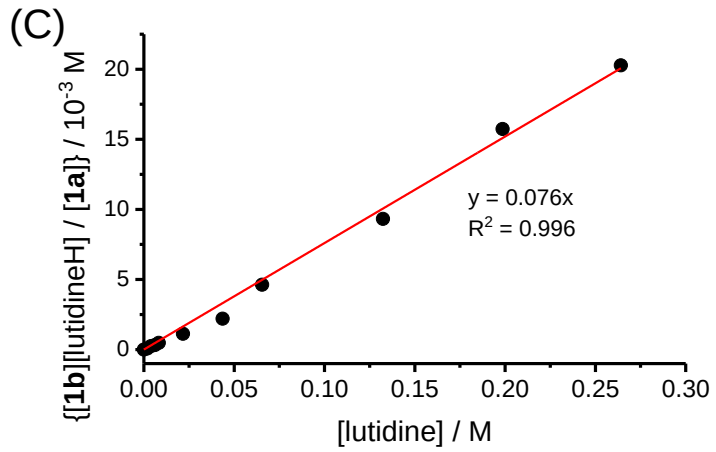

In acetonitrile, **1a** deprotonated quantitatively with DMAP (see Figure 3). The chemical shift of pyrazole proton at 6.36 ppm shifted to 6.11 ppm. The chemical shift of the pyrazole proton for **1a** ($\delta_{\mathbf{1a}}$) and **1b** ($\delta_{\mathbf{1b}}$) were determined as 6.36 and 6.11 ppm, respectively. The proportion of **1a** to the total concentration of ruthenium complexes was calculated from the equation:

$$\frac{[\mathbf{1a}]}{[\mathbf{1a}]+[\mathbf{1b}]} = \left|\frac{\delta_{\text{obsd}} - \delta_{\mathbf{1b}}}{\delta_{\mathbf{1a}} - \delta_{\mathbf{1b}}}\right|$$

where δ_{obsd} is the observed chemical shift. In the titration experiment with lutidine (pK_a = 14.13[2]), the pK_a value of **1a** was determined from the linear plot of [**1b**][lutidineH] / [**1a**] versus [lutidine].[3] The concentrations of lutidine and protonated lutidine (lutidineH) were assumed to be equal. The slope of the line represents an equilibrium constant value of K = 0.076

where:

$$K = \frac{[\mathbf{1b}][\text{lutidineH}]}{[\mathbf{1a}][\text{lutidine}]}$$

The pK was 1.12, which corresponds to the difference of pK_a values of **1a** and lutidine. The pK_a of **1a** was determined to be 15.2.

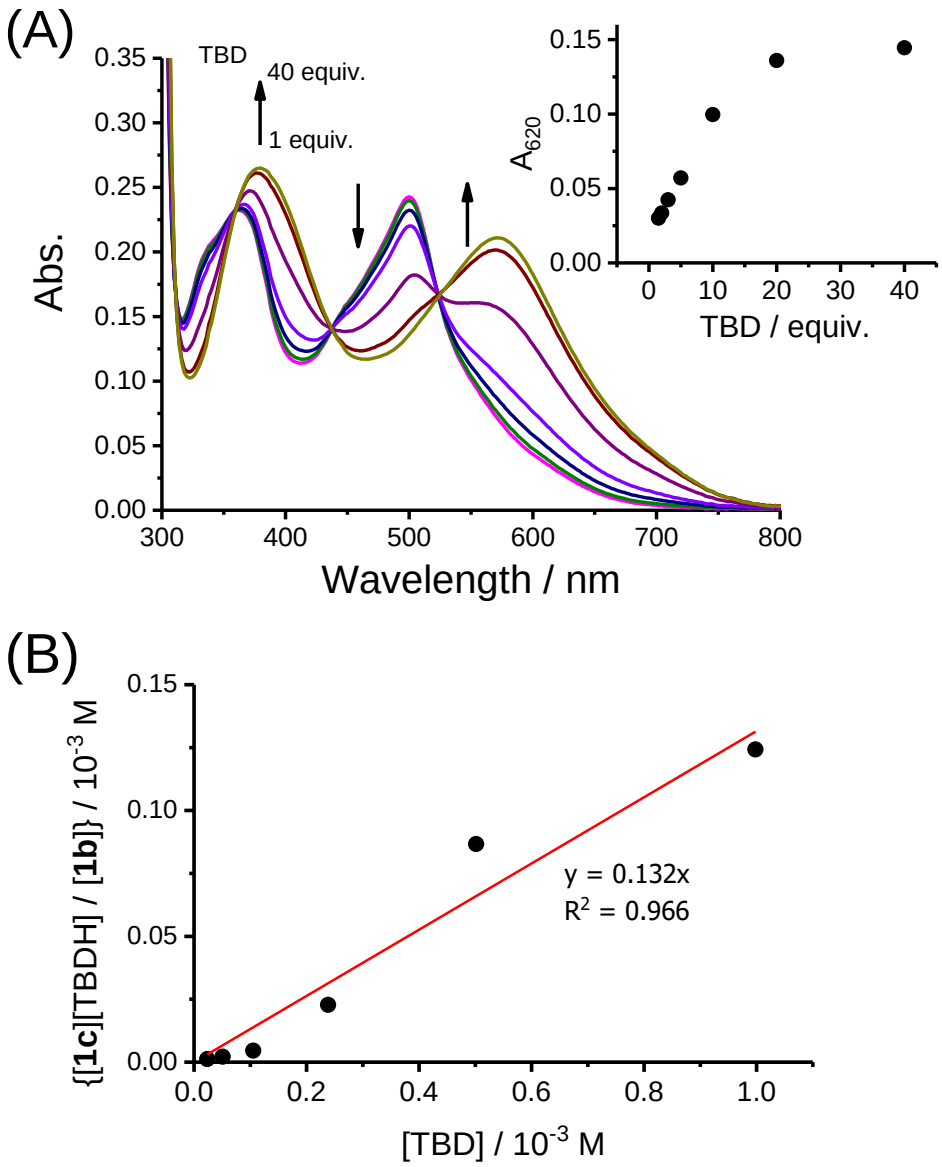

Figure S4. (A) Absorption spectral changes of **1b** during the titration experiments with TBD in MeCN. Inset shows the changes of absorption at 620 nm upon addition of TBD (pK_a = 26.03). The absorption maxima (572 nm) of neutral complex is close to the reported value of neutral complex **1c** (581 nm) in DMF. (B) Titration plot for deprotonation of **1b** to **1c** upon addition with TBD

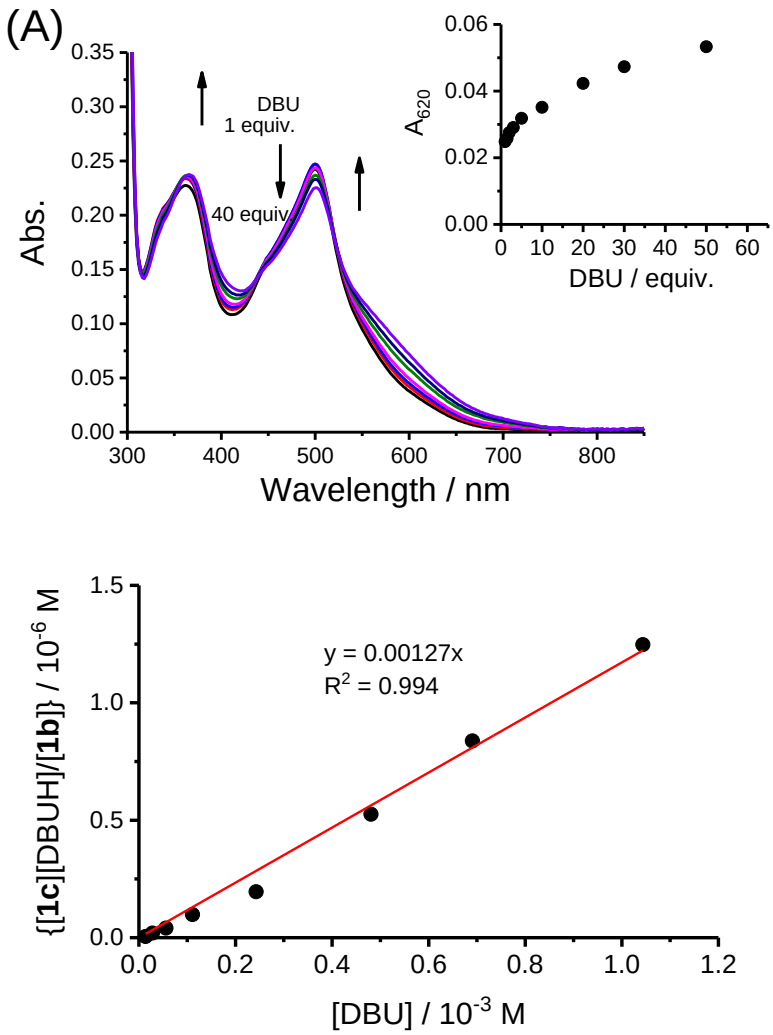

Figure S5. (A) Absorption spectral changes of **1b** during the titration experiments with DBU in MeCN. Inset shows the changes of absorption at 620 nm upon addition of DBU (pK_a = 24.34). (B) Titration plot for deprotonation of **1b** to **1c** upon addition with DBU.

Determination of pK_a value by absorption spectroscopy

The pK_a value of **1b** was determined from absorption spectroscopy instead of ^{1}H NMR spectroscopy due to the poor solubility of **1c**. The proportion of **1b** was calculated from the following equation:

$$\frac{[\mathbf{1b}]}{[\mathbf{1b}]+[\mathbf{1c}]} = \left|\frac{A_{\mathrm{inf}} - A_{\mathrm{obsd}}}{A_{\mathrm{inf}} - A_0}\right|$$

where A_{inf}, A_{obsd}, A_0 were absorbance of **1c** in the presence of 500 equivalents of TBD (pK_a = 26.09[2]), observed absorbance during the titration experiment, initial absorbance of **1b** before titration. The pK_a value of **1b** was determined from the linear plot of [**1c**][TBDH] / [**1b**] versus [TBD].[3] The concentrations of TBD and protonated TBD (TBDH) were assumed to be equal. The slope of the line represents an equilibrium constant value of K = 0.132 as shown in Figure S4B.

where:

$$K = \frac{[\mathbf{1c}][\mathrm{TBDH}]}{[\mathbf{1b}][\mathrm{TBD}]}$$

The pK was 0.88, which corresponds to the difference of pKa values of **1b** and TBD. The pK_a of **1b** was determined to be 26.9.

The titration experiments were carried out with DBU (pK_a = 24.34[2]) (Figure S5). In the same manner, The pK_a value of **1b** was determined from the linear plot of [**1c**][DBUH] / [**1b**] versus [DBU]. The slope of the line represents an equilibrium constant value of K' = 0.00127

where:

$$K' = \frac{[\mathbf{1c}][\mathrm{DBUH}]}{[\mathbf{1b}][\mathrm{DBU}]}$$

The pK was 2.89, which corresponds to the difference of pK_a values of **1b** and DBU. The pK_a of **1b** was estimated to be 27.2, which approximately coincides with the pK_a value of 26.9 estimated from the titration with TBD.

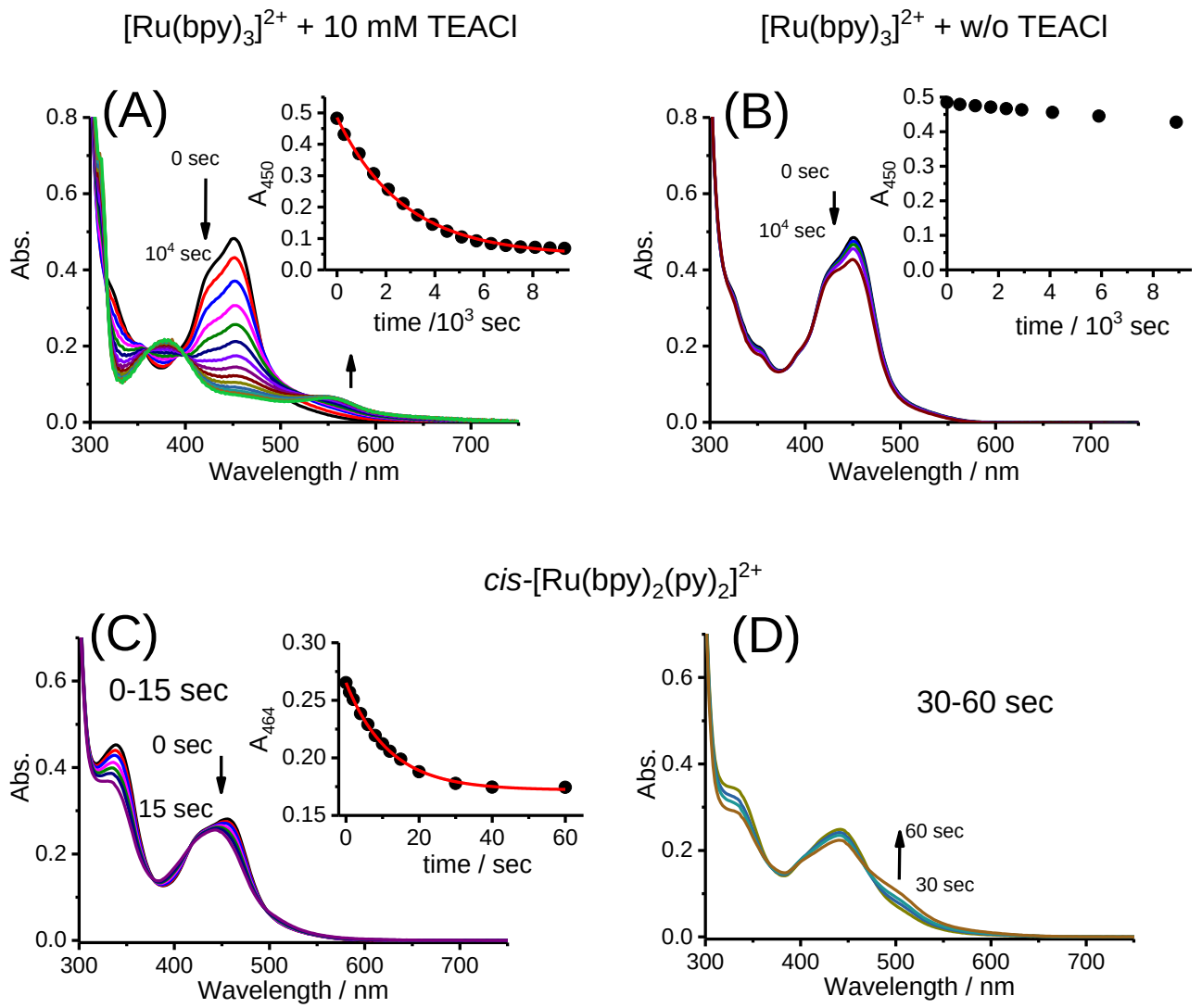

Figure S6. Absorption spectra of (A) $[Ru(bpy)_3]^{2+}$ (32 μM) and TEACl (10 mM), (B) $[Ru(bpy)_3]^{2+}$ (32 μM), (C) *cis*-$[Ru(bpy)_2(py)_2]^{2+}$ (0-15sec), and (D) *cis*-$[Ru(bpy)_2(py)_2]^{2+}$ (30-60 sec) during photolysis with blue LED (λ = 470 nm, 14 mW cm^{-2}) in acetonitrile containing 10 mM TEACl at 298 K. Insets in Figure S7(C) show kinetic traces based on the absorbance changes (black dots) and fitting curves (red line).

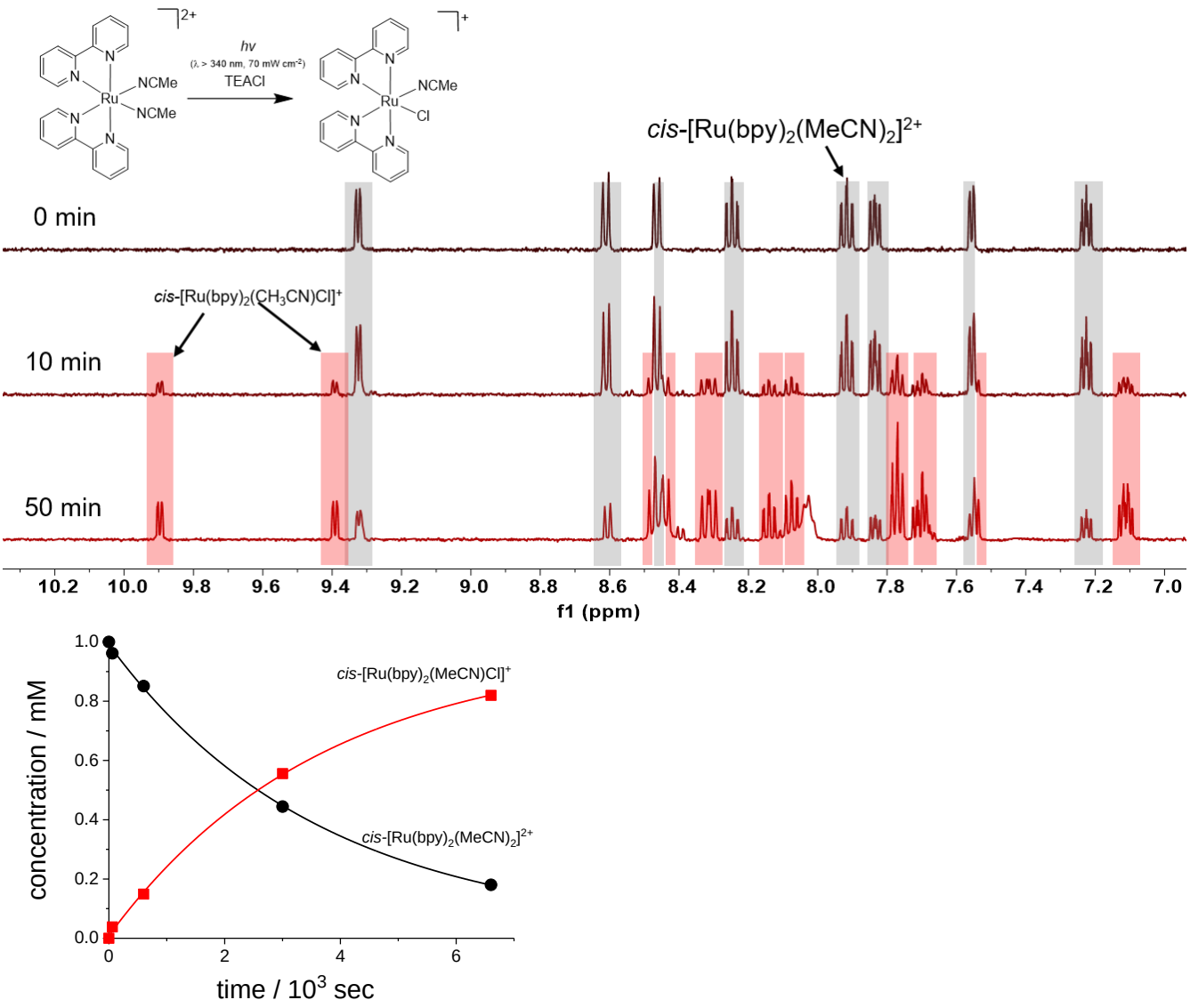

Figure S7. (A) ^{1}H NMR spectra of *cis*-$[Ru(bpy)_2(MeCN)_2]^{2+}$ (1.0 mM), during photolysis with polychromatic light (λ > 340 nm, 70 mW cm^{-2}) in CH_3CN and CD_3CN (CH_3CN : CD_3CN = 1:1) containing 10 mM TEACl. Peaks of *cis*-$[Ru(bpy)_2(MeCN)_2]^{2+}$ and *cis*-$[Ru(bpy)_2(MeCN)Cl]^{+}$ are highlighted with gray and red, respectively. (B) Kinetic traces of *cis*-$[Ru(bpy)_2(MeCN)_2]^{2+}$ (black) and *cis*-$[Ru(bpy)_2(MeCN)Cl]^{+}$ (red), where the concentrations of the reactant and product were calculated based on the integrations at 9.33 and 9.38 ppm, respectively.

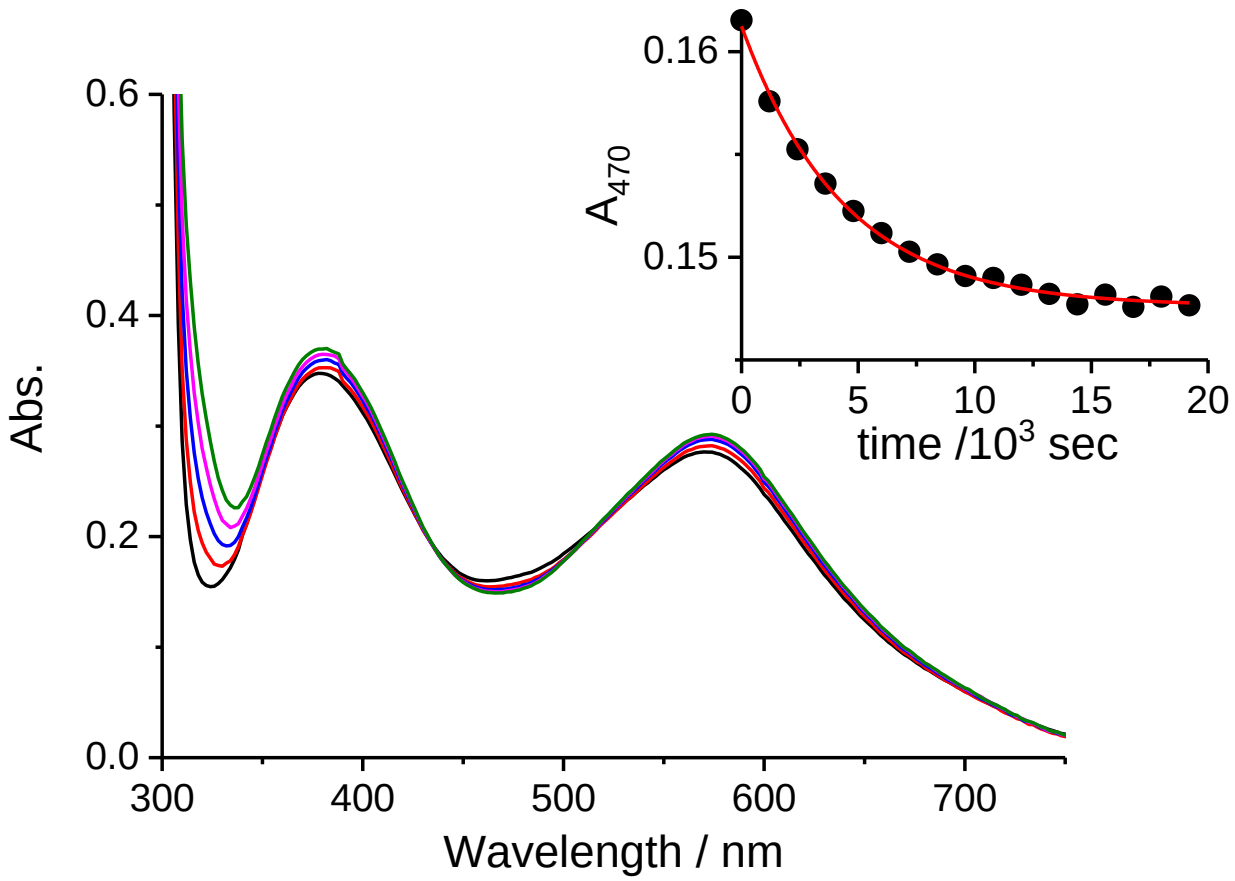

Figure S8. Absorption spectra of **1c** (37 μM) and TBD (16 mM) during photolysis with blue LED (λ = 470 nm, 14 mW cm^{-2}) in acetonitrile containing 10 mM TEACl. Insets show kinetic traces based on the absorbance changes (black dots) and fitting curves (red line).

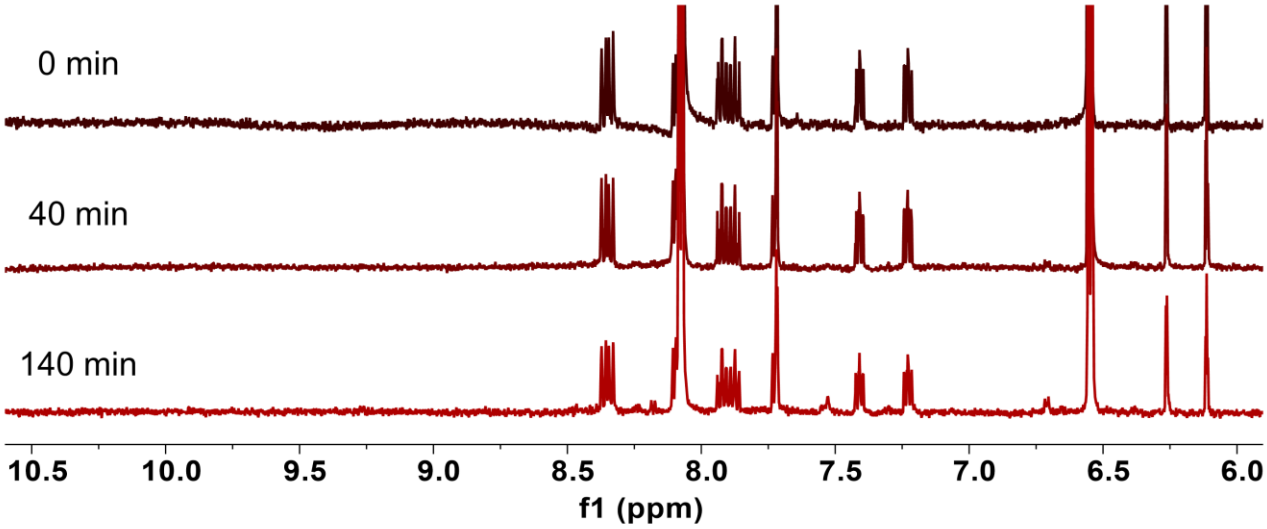

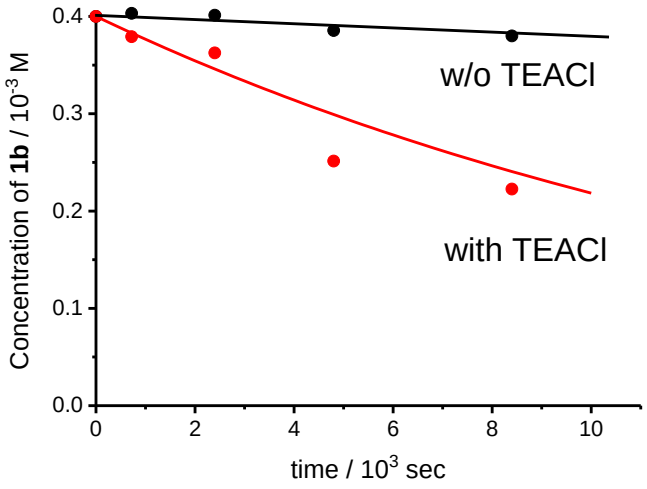

Figure S9. (A) ^{1}H NMR spectra of **1b** (0.4 mM), during photolysis with polychromatic light (λ > 340 nm, 70 mW cm^{-2}) in acetonitrile/CD_3CN containing 4 mM DMAP. (B) Kinetic traces of **1b** during photolysis in the absence (black) and presence (red) of TEACl. The concentration of **1b** was calculated based on the integrations of the peak at 7.22 ppm.

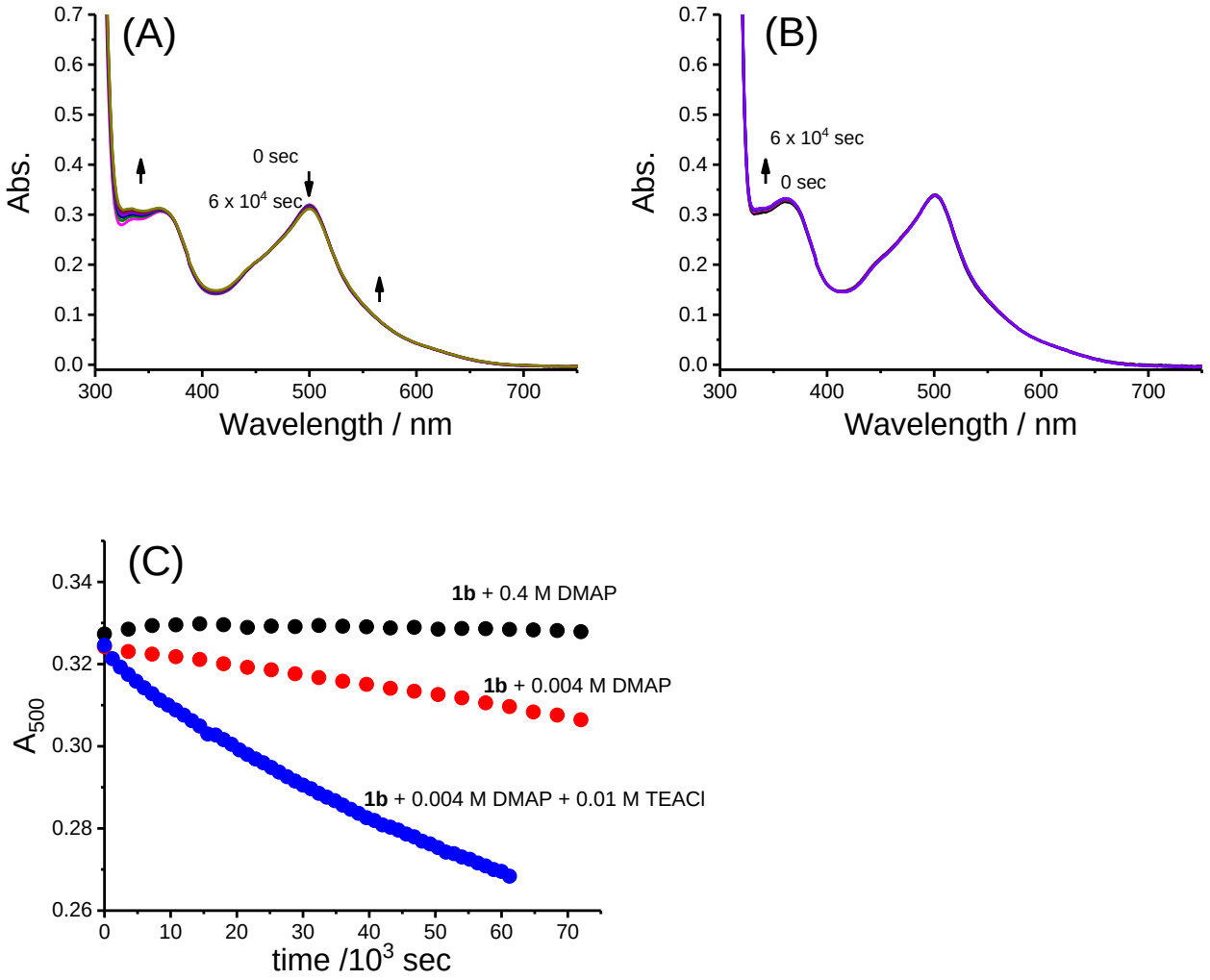

Figure S10. Absorption spectra of (A) **1b** (38 μM) with 4 mM DMAP and (B) **1b** (38 μM) with 0.4 M DMAP during photolysis with blue LED (λ = 470 nm, 14 mW cm^{-2}) in the absence of TEACl in acetonitrile. The increase of absorbance below 340 nm may be an absorption band of protonated DMAP ($DMAPH^+$), [4] which was formed overtime by the protonation with trace amount of water. (C) Kinetic traces of **1b** based on the absorbance changes at 540 nm in the presence of 0.4 M DMAP (black), 4 mM DMAP (red), and 4 mM DMAP and 0.01 M TEACl (blue).

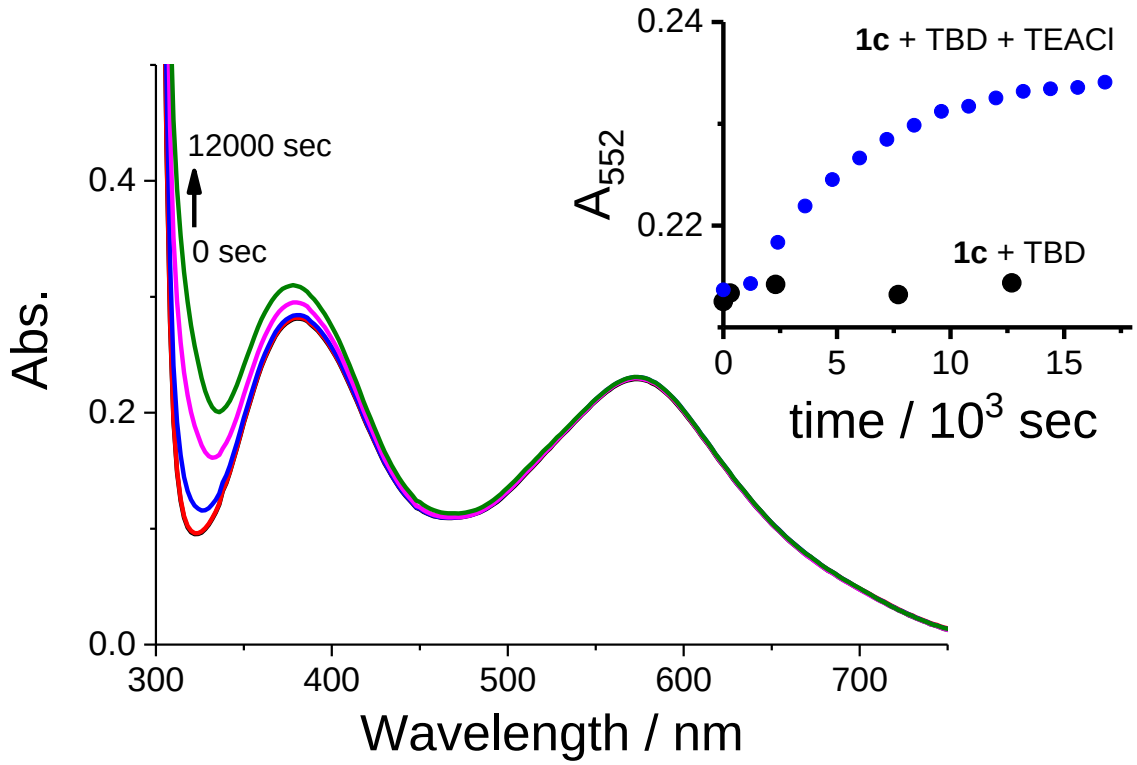

Figure S11. Absorption spectra of **1c** (33 μM) and TBD (10 mM) during photolysis with blue LED (λ = 470 nm, 14 mW cm^{-2}) in acetonitrile. Inset shows kinetic traces base on the absorbance changes at 552nm of the sample solution containing **1c** and TBD (black) and **1c**, TBD, and TEACl (blue)

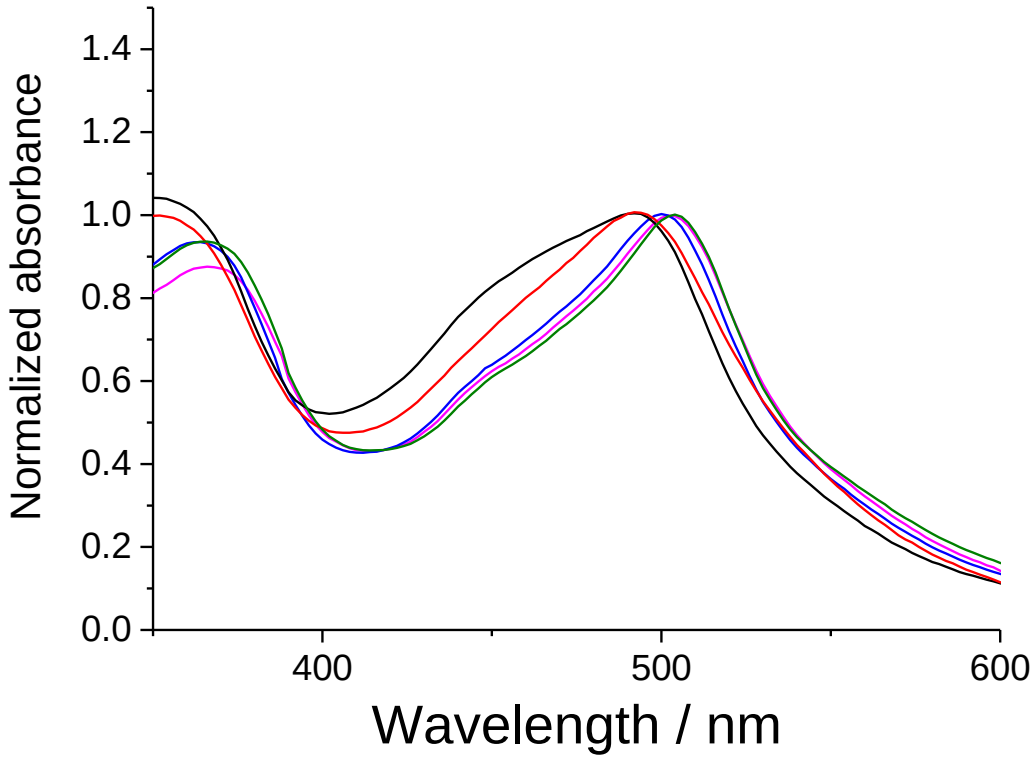

Figure S12. Normalized absorption spectra of **1b** in TFE (black), water (red, pH = 12), MeCN (blue), DMSO (cyan) , and MeOH (green).

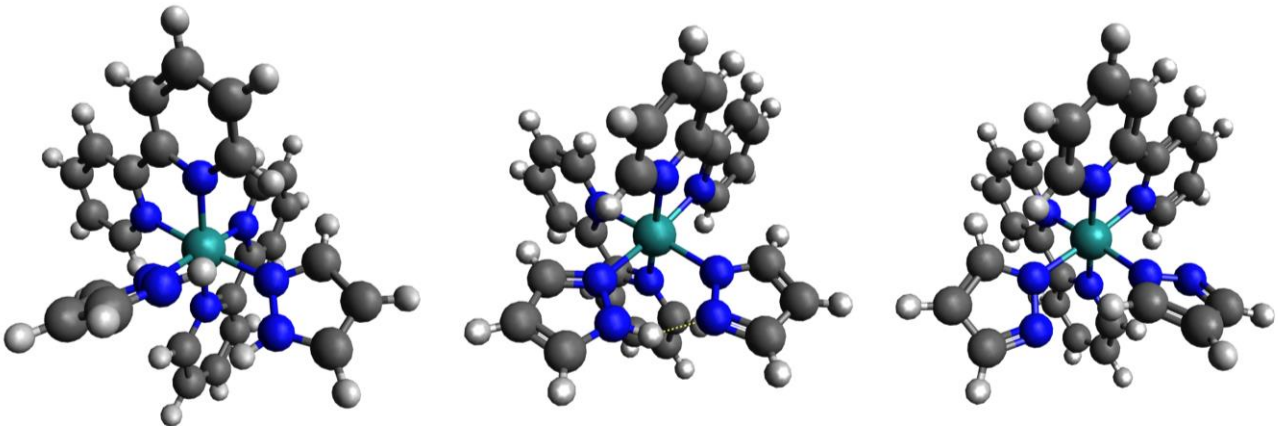

Figure S13. Optimized structures of **1a** (left), **1b** (center), and **1c** (right), which were optimized at the B3LYP level of DFT using LanL2DZ basis set in Gaussian 09.

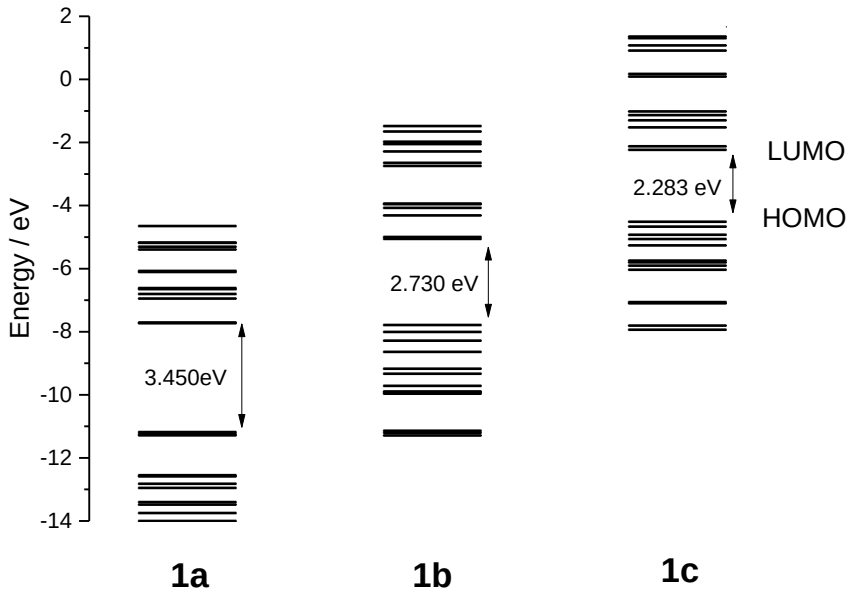

Figure S14. Energy level diagram of molecular orbitals (HOMO–12 to LUMO+12) of **1a**, **1b**, and **1c**. Complex geometries were fully optimized under gaseous conditions using the B3LYP method.

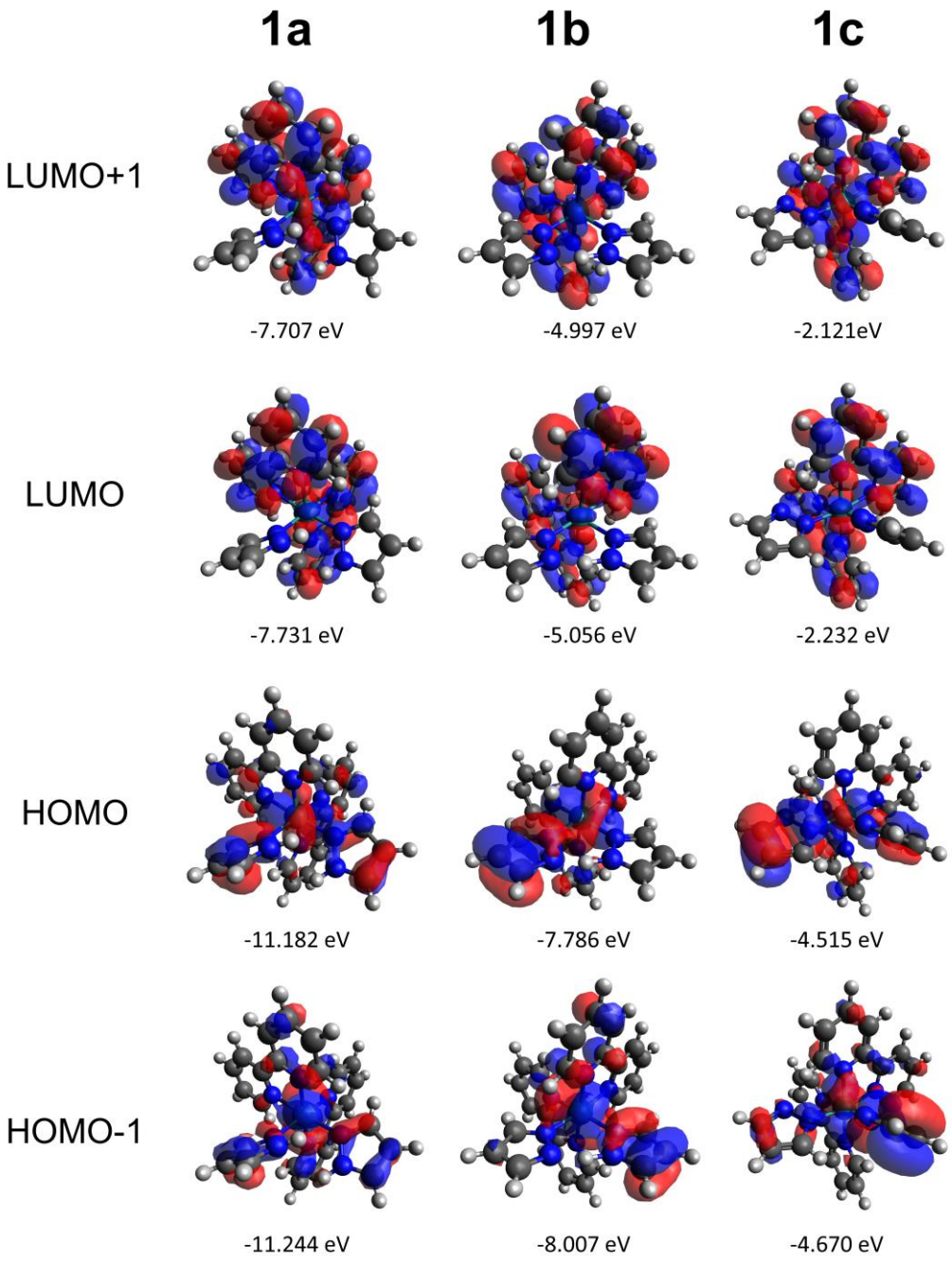

Figure S15. Frontier molecular orbitals of **1a**, **1b**, and **1c**.

Table S1. Selected crystallographic parameters

compounds	[**1a**]$(CF_3SO_3)_2$	[**1b**](PF_6)
empirical formula	$RuS_2F_6O_6N_8C_{28}H_{24}$	$RuPF_6N_8C_{26}H_{23}$
fw	847.74	693.56
radiation	Mo Kα	Mo Kα
crystal system	monoclinic	orthorhombic
space group	*C2/c*	$P2_12_12_1$
a, Å	22.637(10)	11.9435(2)
b, Å	11.256(5)	12.3203(2)
c, Å	16.144(13)	18.0256(3)
α, deg	90	90
β, deg	128.144(4)	90
γ, deg	90	90
V, Å^3	3235(3)	2652.42(8)
Z	4	4
μ, mm^{-1}	0.705	0.728
T, K	100	100
d_{cal}, g/cm^3	1.741	1.737
T_{min}, T_{max}	0.5844, 0.7456	0.711, 0.745
N_{ref}	3712	5236
$R[F^2 > 2\sigma(F^2)]$	0.0632	0.0173
$wR[F^2 > 2\sigma(F^2)]$	0.1076	0.0429
GOF	1.0195	1.054

Table S2 Selected bond distances (Å) and angles (°)

	[**1a**]$(CF_3SO_3)_2$	[**1b**](PF_6)
$Ru1\text{-}N1_{bpy}$	2.057(5)	2.0696(16)
$Ru1\text{-}N1_{bpy}$	2.065(4)	2.0552(16)
$Ru1\text{-}N3_{pzH}$	2.087(5)	
$Ru1\text{-}N3_{bpy}$		2.0482(15)
$Ru1\text{-}N4_{bpy}$		2.0510(16)
$Ru1\text{-}N5_{pzH}$		2.0917(17)
$Ru1\text{-}N7_{pz}$		2.0960(15)
$N1_{bpy}\text{-}Ru1\text{-}N1_{bpy}$	89.9(3)	
$N1_{bpy}\text{-}Ru1\text{-}N2_{bpy}$	79.12(18), 95.02(18)	97.13(17)
$N1_{bpy}\text{-}Ru1\text{-}N3_{pzH}$	176.27(18), 90.26(16)	
$N2_{bpy}\text{-}Ru1\text{-}N2_{bpy}$	171.8(3)	
$N2_{bpy}\text{-}Ru1\text{-}N3_{pzH}$	88.68(17), 97.15(18)	
$N3_{pzH}\text{-}Ru1\text{-}N3_{pzH}$	89.8(3)	
$N1_{bpy}\text{-}Ru1\text{-}N3_{bpy}$		174.66(6)
$N1_{bpy}\text{-}Ru1\text{-}N4_{bpy}$		98.84(6)
$N1_{bpy}\text{-}Ru1\text{-}N5_{pzH}$		85.30(6)
$N1_{bpy}\text{-}Ru1\text{-}N7_{pz}$		97.28(6)
$N2_{bpy}\text{-}Ru1\text{-}N3_{bpy}$		96.08(6)
$N2_{bpy}\text{-}Ru1\text{-}N4_{bpy}$		87.62(6)
$N2_{bpy}\text{-}Ru1\text{-}N5_{pzH}$		91.94(6)
$N2_{bpy}\text{-}Ru1\text{-}N7_{pz}$		174.70(6)
$N3_{bpy}\text{-}Ru1\text{-}N4_{bpy}$		174.70(6)
$N3_{bpy}\text{-}Ru1\text{-}N5_{pzH}$		96.72(6)
$N3_{bpy}\text{-}Ru1\text{-}N7_{pz}$		87.63(6)
$N4_{bpy}\text{-}Ru1\text{-}N5_{pzH}$		175.66(6)
$N4_{bpy}\text{-}Ru1\text{-}N7_{pz}$		89.38(6)
$N5_{pzH}\text{-}Ru1\text{-}N7_{pz}$		91.37(6)
$N4_{pzH}\bullet\bullet\bullet N4_{pzH}$	3.180(9)	
$N6_{pzH}\bullet\bullet\bullet N8_{pz}$		2.623(2)

References

(1) Sullivan, B. P.; Salmon, D. J.; Meyer, T. J.; Peedin, J. Monomeric and dimeric pyrazole and pyrazolyl complexes of ruthenium. *Inorg. Chem.* **1979**, *18*, 3369-3374.

(2) Kaljurand, I.; Kütt, A.; Sooväli, L.; Rodima, T.; Mäemets, V.; Leito, I.; Koppel, I. A. Extension of the Self-Consistent Spectrophotometric Basicity Scale in Acetonitrile to a Full Span of 28 pKa Units: Unification of Different Basicity Scales. *The Journal of Organic Chemistry* **2005**, *70*, 1019-1028.

(3) Reed, C. J.; Agapie, T. Thermodynamics of Proton and Electron Transfer in Tetranuclear Clusters with Mn–OH_2/OH Motifs Relevant to H_2O Activation by the Oxygen Evolving Complex in Photosystem II. *J. Am. Chem. Soc.* **2018**, *140*, 10900-10908.

(4) Mishina, S.; Takayanagi, M.; Nakata, M.; Otsuki, J.; Araki, K. Dual fluorescence of 4-dimethylaminopyridine and its derivatives: Effects of methyl substitution at the pyridine ring. *J. Photochem. Photobiol. A-Chem.* **2001**, *141*, 153-158.